New Phytologist

Research

Plant functional trait uncertainty can outweigh climate scenario uncertainty in tundra ecosystem productivity

Katya R. Jay[1,2], William R. Wieder[1,3], Sarah C. Elmendorf[1,4], Marko J. Spasojevic[5] and Katharine N. Suding[1,4]

[1]Institute of Arctic and Alpine Research, University of Colorado, 4001 Discovery Dr., Boulder, CO 80303, USA; [2]Cooperative Institute for Research in Environmental Sciences, University of Colorado, 1665 Central Campus Mall 216 UCB, Boulder, CO 80309, USA; [3]Climate and Global Dynamics Laboratory, National Center for Atmospheric Research, Box 3000, Boulder, CO 80307, USA; [4]Department of Ecology and Evolutionary Biology, University of Colorado, 1900 Pleasant St., Boulder, CO 80302, USA; [5]Department of Evolution, Ecology, and Organismal Biology, University of California Riverside, 2710 Life Science Building, Riverside, CA 92521, USA

Author for correspondence:
Katya R. Jay
Email: katya.jay@colorado.edu

Received: *23 June 2025*
Accepted: *23 October 2025*

New Phytologist (2025)
doi: 10.1111/nph.70740

Key words: climate change, Community Land Model, plant functional traits, trait variation, tundra.

Summary

- Predicting shifts in species composition with global change remains challenging, but plant functional traits provide a key link to scale from plant to community and ecosystem levels. The extent to which functional trait shifts may mediate ecosystem response to climate change remains a critical question.
- We ran point-scale Community Land Model (CLM) simulations with site-specific functional trait and phenology observations to represent alpine tundra growth strategies. We validated our results with site observations and compared parameterized results to those using the default parameterization. We then quantified the relative contribution of plant functional trait shifts vs climate change scenarios (and the resulting phenological shifts) to uncertainty in future tundra ecosystem productivity outcomes.
- We found that using community-specific functional traits and phenology observations significantly improved productivity estimates compared with overestimates in a default simulation. Uncertainty in potential plant trait shifts often had a larger effect on ecosystem productivity responses than uncertainty in the forced response from different climate change scenarios.
- These findings highlight the key role of functional traits in shaping vegetation responses to climate change and the value of incorporating site-level measurements into land models to more accurately forecast climate change impacts on ecosystem function.

Introduction

Predictions of climate change impacts on terrestrial ecosystems remain highly uncertain. Yet, terrestrial vegetation moderates land–atmosphere interactions by shaping water, carbon (C), and energy fluxes (Bonan, 2008; Verheijen *et al.*, 2013), making it essential to better understand how vegetation responds to climate change and how these vegetation responses moderate changes in ecosystem function. Rates of vegetation change can be fast, closely tracking climate change, or slow, lagging climate changes and leading to disequilibria (Williams *et al.*, 2021). Consideration of shifts in plant functional traits provides a critical link to integrate species and community responses to environmental change factors (Suding *et al.*, 2008; Pacifici *et al.*, 2017). Plant functional traits (characteristics that influence growth, reproduction, and survival), particularly those linked to the resource economics spectrum (Wright *et al.*, 2004), are indicative of a plant's ecological strategies. These traits have been used to predict community responses to environmental change and have been linked to ecosystem processes, including nutrient cycling, C storage, and productivity (Funk *et al.*, 2017; He *et al.*, 2023).

Combinations of functional traits can determine whether plants have more resource-use conservative or acquisitive growth strategies as they balance growth potential and longevity against leaf construction costs. For example, plants with more resource-acquisitive strategies tend to exhibit faster growth rates, higher nutrient uptake, and shorter-lived leaves and tissues (Shipley *et al.*, 2006). Accordingly, more resource-acquisitive plants tend to have higher specific leaf area (SLA; the ratio of leaf area to leaf dry mass); lower water use efficiency, inferred from C isotope discrimination (lower $\delta^{13}C$); higher leaf nitrogen (N) content; and lower leaf C : N ratios than plants with more resource-conservative growth strategies (Reich, 2014; Díaz *et al.*, 2016). Responses of vegetation to warming are likely to include shifts in these functional traits due to changes in species composition or relative abundance as a result of adaptation, phenotypic plasticity, or compositional turnover (Moritz & Agudo, 2013; Bjorkman *et al.*, 2018). Beyond these functional

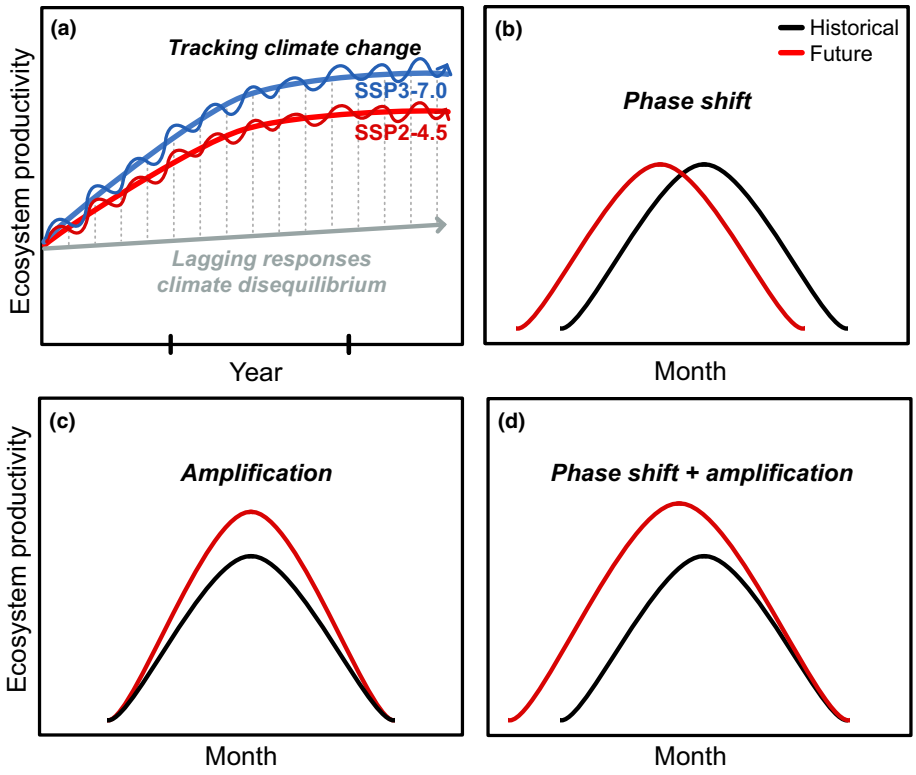

Fig. 1 Hypothesized ecosystem productivity responses to climate change depend on the rate of abiotic change (e.g. warming) and associated biotic responses. The extent of abiotic change is associated with forcing uncertainty from different climate change scenarios, with increasing emissions and atmospheric CO_2 concentrations, illustrated on the *x*-axis in (a). Biotic responses to climate change may include (a) phenotypic plasticity and community turnover, leading to plant functional trait changes that track rates of climate change, maintaining optimal productivity of the system (blue and red lines represent a hypothesized productivity response under Shared Socioeconomic Pathways (SSP) scenarios, SSP2-4.5 and SSP3-7.0, respectively, and wavy blue and red lines represent a system that is keeping pace with climate change as a result of functional trait changes under the two scenarios). Climate disequilibria can occur when rates of ecosystem responses lag behind the rate of climate change (represented by the gray line, with dashed lines representing productivity differences due to disequilibrium). Plant community responses that may facilitate ecosystem tracking of abiotic change could include: (b) climate-driven phenological changes (e.g. from earlier snow melt) that lead to a phase shift in the annual cycle of productivity; (c) amplification of the annual cycle of productivity due to improved growing conditions or potential functional trait responses toward more resource-acquisitive growth strategies; or (d) interacting phenology and functional trait shifts that drive a phase shift and amplification of ecosystem productivity.

traits, plant phenology, including the timing of leaf onset and senescence, is also likely to shift with warming, leading to potential mismatches between vegetation productivity and resource availability (Cleland *et al.*, 2007). Together, vegetation responses to warming will likely result in changes in both functional traits and phenology, but the rate of change of these shifts and their effect on ecosystem function remains highly uncertain.

In addition to shaping plant growth strategies, functional traits provide a mechanistic link between plant communities and ecosystem processes and can play a key role in shaping rates of ecosystem productivity (Tilman *et al.*, 2001; Hooper *et al.*, 2005; Huxley *et al.*, 2023). In a global analysis pairing flux tower measurements with extrapolated future plant trait maps, Madani *et al.* (2018) found strong relationships between local environmental conditions and plant traits, including SLA and height, suggesting that increasing plant height and SLA will accompany increases in gross primary productivity (GPP) under future climate conditions. However, the pace of functional trait responses to climate change can range from days to decades or centuries, meaning that ecosystem responses can either track or lag behind the rate of climate change. This may result in novel combinations of abiotic climate conditions and functional traits (Fig. 1a; Svenning & Sandel, 2013; Butler *et al.*, 2017; Felton *et al.*, 2022), that together impact the magnitude and timing of plant productivity. For example, where leaf out is stimulated by warming or earlier snowmelt we might expect to see a phase shift in productivity in response to climate change (Fig. 1b). Shifts in plant functional traits toward more resource-acquisitive growth strategies could amplify productivity responses to climate change (Fig. 1c). Finally, interactions between phenological and functional trait changes could result in phase shifts and amplification of ecosystem processes that would facilitate tracking of changing climate conditions (Fig. 1d; also see Butterfield *et al.*, 2020 for evidence of productivity amplification and seasonal phase shifts in response to interannual climate variability). Previous work suggests that the magnitude of climate disequilibrium is a large source of uncertainty in projections of future herbaceous net primary productivity (NPP), outweighing uncertainties among

different climate models and emissions pathways (Felton *et al.*, 2022). Because the potential impacts of these climate disequilibria on ecosystem functions are not well understood, more work is needed to quantify how uncertainty in changes in plant traits may lead to tracking or lagging ecosystem responses to abiotic change.

High-elevation and high-latitude regions are warming more rapidly than other regions of the globe (Wang *et al.*, 2016; Rantanen *et al.*, 2022), making alpine and arctic tundra ecosystems particularly vulnerable to climate change. Increasing temperatures in tundra ecosystems leads to accelerated snowmelt, shifts in phenology, and altered nutrient cycling (Walker *et al.*, 2006; Dong *et al.*, 2019; Wieder *et al.*, 2022), but predicting responses to these synergistic changes remains a challenge. Some studies suggest that alpine plant communities have shifted toward more resource-conservative, stress-tolerant functional traits (e.g. lower SLA and higher water-use efficiency) with warming over the past several decades (Huxley & Spasojevic, 2021; Oldfather *et al.*, 2024). Other analyses of tundra global change experiments and syntheses of long-term observations show increases in resource-acquisitive traits such as SLA with warming (Bjorkman *et al.*, 2018; Henn *et al.*, 2024). Because functional traits are strong predictors of ecosystem productivity (Madani *et al.*, 2018), we expect these potential shifts in traits to alter patterns of productivity across tundra ecosystems. This type of ecological uncertainty, however, rarely factors into physical climate change projections that focus on natural variability (internal variability in the climate system), model structural uncertainty, and scenario uncertainty (uncertainty in future emissions and climate change trajectories; Hawkins & Sutton, 2009; Bonan *et al.*, 2019). Thus, approaches quantifying the relative contribution of trait uncertainty, which may contribute to climate disequilibria, in shaping ecosystem responses to climate change are needed, especially in comparison to other sources of uncertainty.

To better understand ecosystem sensitivity to plant functional trait responses that may lag behind or track climate change, we used local site observations to parameterize a land model to represent tundra vegetation communities and examined changes in productivity under two future climate scenarios. We used the Community Land Model v.5 (CLM5; Lawrence *et al.*, 2019) with a hillslope hydrology configuration (Swenson *et al.*, 2019) to run single-point simulations that represent water, energy, C, and nutrient fluxes at the Niwot Ridge Long Term Ecological Research (LTER) site. We modified CLM parameters representing functional traits and phenology using site observations, evaluated our simulations against site observations, and compared our simulations with one using default values of functional traits and phenology. We then extended our model simulations through the end of this century with modified functional trait configurations that represent shifts toward more resource-use conservative or acquisitive communities that encompass a range of potential trait responses that could track or lag climate change (Fig. 1). We ran these future simulations under two climate change scenarios, which are coupled with phenological changes because leaf onset in CLM is controlled by soil temperature. This allowed us to assess the relative contribution of uncertainty in trait responses to that of climate scenario uncertainty in shaping productivity responses under climate change. Specifically, we hypothesized that: (1) shifts in functional traits, climate scenarios, and phenology will interact, leading to both amplification and phase shift responses in productivity (Fig. 1d); and (2) the relative contributions of functional trait uncertainty vs climate scenario uncertainty to tundra productivity will be mediated by resource availability across tundra communities. By quantifying both functional trait and climate scenario uncertainties, our study elucidates the importance of plant trait responses in shaping ecosystem responses to climate change.

Materials and Methods

Study site and local site observations

This study focuses on Niwot Ridge, Colorado (CO), USA (40°03′N, 105°35′W, *c.* 3500 m asl), a high-elevation alpine tundra site in the CO Rocky Mountains, USA. Climate records from 1953 to present show a strong warming trend at this site, particularly in spring and summer months, with maximum annual temperatures increasing at *c.* 0.5°C per decade (Kittel *et al.*, 2015). Because most precipitation falls as snow at this site (*c.* 80%; Caine, 1996), plants experience a short growing season of *c.* 2–3 months. Due to the topographically variable nature of alpine terrain, snow is redistributed by wind, with some areas accumulating a deep snowpack while others remain wind-blown and snow-free (Winstral *et al.*, 2002; Erickson *et al.*, 2005; Litaor *et al.*, 2008; Mott *et al.*, 2018). This gradient in snow accumulation is a key factor driving variation in community composition and productivity in tundra vegetation. Wind-blown areas with little or no snow cover typically host dry meadow or fellfield communities with shallow, rocky soils, and low statured vegetation that tends to be less productive (Billings & Mooney, 1968). Moist meadow vegetation occurs in areas with deep snow accumulation that provides higher soil moisture content and productivity. Wet meadow vegetation is found in lowland areas that receive snowmelt from upslope as runoff and have the highest productivity (Walker *et al.*, 2001).

Foliar traits and phenology To characterize differences in plant functional traits among tundra vegetation communities at our site, we used functional trait data collected at Niwot Ridge. We calculated community-weighted mean trait values of SLA, leaf C : N, and $\delta^{13}C$ using species mean trait values from published trait data for moist, wet, and dry meadow vegetation at Niwot Ridge (Fig. 2; Spasojevic & Suding, 2012; Spasojevic *et al.*, 2013, 2022).

To characterize phenological differences among tundra communities, we leveraged a dataset of phenocam images collected half-hourly throughout the growing season from 2018 to 2022 at plots in the Niwot Ridge Sensor Network Array (Morse & Niwot Ridge LTER, 2022). Green chromatic coordinate (GCC) values were extracted from these images at each plot taken between 09:00 and 13:00 h (Elwood *et al.*, 2022) and categorized as moist, wet, or dry meadow based on the dominant plant community. We then derived a suite of phenometrics from these GCC

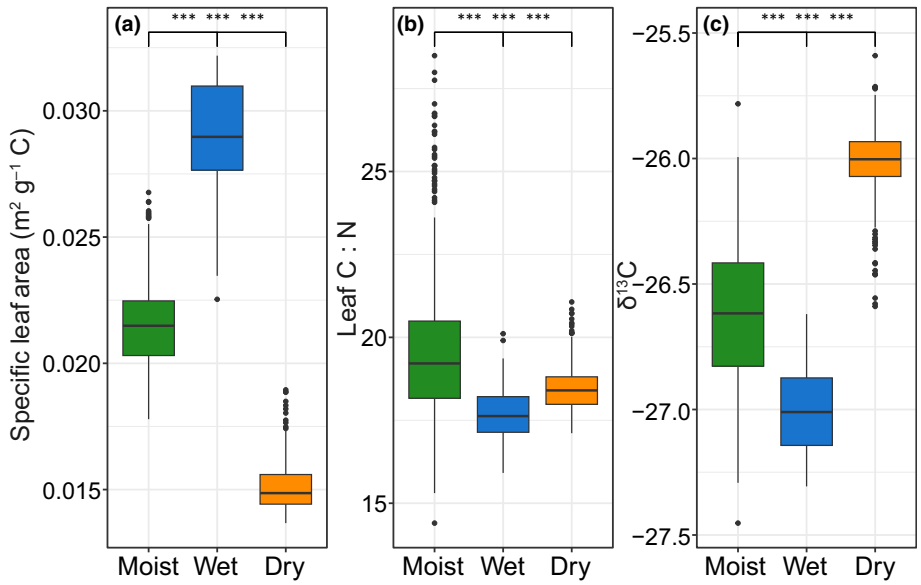

Fig. 2 Box-and-whisker plots showing the median, interquartile range, and range of plant foliar trait values by community. (a) Specific leaf area (m^2 g^{-1} C), (b) leaf C : N ratio, (c) $\delta^{13}C$. Moist, wet, and dry meadow communities are shown in green, blue, and orange, respectively. ***, $P < 0.001$ in Kruskal–Wallis test with Bonferroni–Dunn *post hoc* corrections.

values that characterize the timing and length of the growing season. To derive these phenometrics, we first determined the spring snowmelt date either by observing it directly in the images or by using 5 cm soil temperature probes to determine the first day in spring when the 5-d running mean diurnal soil temperature exceeded the (plot-specific) value from years where snowmelt was observed (in cases where cameras were deployed shortly after snowmelt). Because fitting curves to snow-free values often gave a poor fit due to the lack of baseline (dormant-season) GCC estimates, we infilled GCC values before spring snowmelt and after fall snow onset. We did this by sampling from a normal distribution with a mean value of plot-specific average 'max GCC' values at snowmelt, averaged over all years, and the corresponding node-specific SD. We then fitted a double-logistic curve (Beck *et al.*, 2006) to the complete seasonal series with a 15 : 1 weighting scheme of observed (non-snow-covered): snow-covered days. We defined the timing of greenup and senescence as the half-maximum of the fitted curves on the rising and falling limbs, respectively, and the peak as the derived peak (Fig. 3a). Additional metrics included the rate of greenup and the rate of senescence (Filippa *et al.*, 2016).

To analyze functional traits and phenology metrics for differences across vegetation communities, we used the Kruskal–Wallis test, a nonparametric alternative to ANOVA that does not assume normality in the data. When significant differences were detected, *post hoc* pairwise comparisons were performed using the Bonferroni–Dunn test. This test adjusts for multiple comparisons, identifying pairwise differences while controlling the family-wise error rate. Results were visualized using boxplots, with the median and interquartile range (IQR) represented by the boxes, whiskers extending to 1.5 times the IQR, and outliers defined as values outside of 1.5 times the IQR.

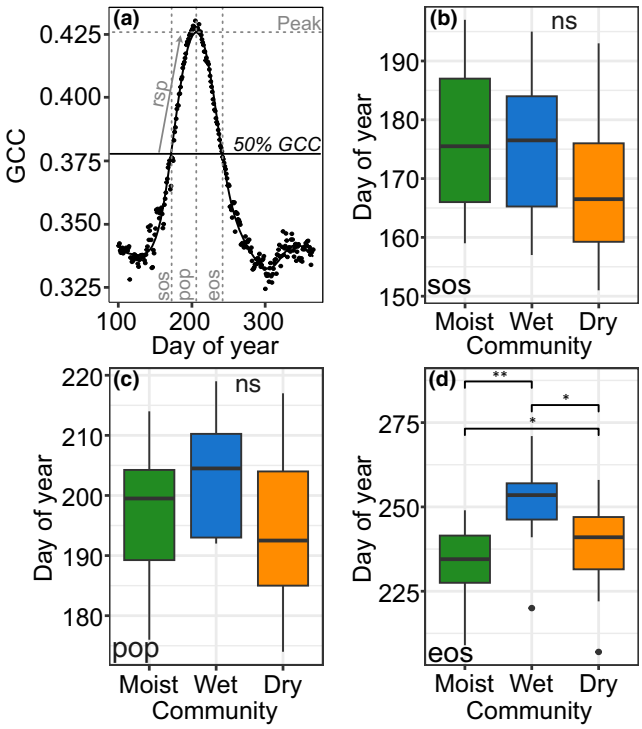

Fig. 3 Box-and-whisker plots showing the median, interquartile range, and range of phenology metrics from moist, wet, and dry meadows in green, blue, and orange, respectively. (a) Example green chromatic coordinate (GCC) curve over one growing season showing phenometrics where they occur; (b) start of season (sos) (day of year; doy); (c) peak of season position (pop) (doy); (d) end of season (eos) (doy). *, $P < 0.05$ and **, $P < 0.01$ in Kruskal–Wallis test with Bonferroni–Dunn *post hoc* corrections. ns, not significant.

Model forcing and evaluation To run and evaluate single-point CLM simulations, we used local observations from a combination of alpine and subalpine stations at Niwot Ridge, following the methods of Jay *et al.* (2023). Meteorological measurements, including air temperature, barometric pressure, relative humidity, and wind speed, are available from two alpine eddy covariance

towers located in fellfield and dry meadow communities at 3480 m asl (AmeriFlux sites US-NR3 and US-NR4; Knowles *et al.*, 2012; Knowles, 2022a,b); we used US-NR4 measurements that were gap-filled with measurements from US-NR3. Because incoming solar measurements were not collected reliably at these high-elevation sites, we used incoming shortwave radiation data from a nearby subalpine eddy covariance tower (Ameriflux site US-NR1, 3050 m asl; Burns *et al.*, 2016). Precipitation data are available from the Saddle site at Niwot Ridge (3525 m asl) as well as the subalpine U.S. Climate Reference Network (USCRN) station 14W (40°02′N, 105°32′W, 3050 m asl; NOAA, 2021). We modified precipitation data from the Saddle site to account for the effects of blowing snow during October–May following Williams *et al.* (1998) and used the half-hourly USCRN record to distribute the Saddle precipitation record to half-hourly measurements as required to run CLM. Finally, we used a variety of publicly available Niwot Ridge datasets to evaluate our model simulations. These included: snow depth collected across 88 gridded points, *c.* biweekly (D. Walker *et al.*, 2022) and corresponding descriptions of dominant plant communities (Spasojevic *et al.*, 2013), aboveground biomass clippings used to estimate annual aboveground net primary productivity (ANPP; M. Walker *et al.*, 2022), and GPP estimates from the alpine flux towers (Knowles, 2022a,b).

CLM overview and site-specific setup

Abiotic heterogeneity We ran single-point simulations using the CLM v.5 (Lawrence *et al.*, 2019), the terrestrial component of the Community Earth Systems Model (CESM; Danabasoglu *et al.*, 2020), with hillslope hydrology (Swenson *et al.*, 2019) and active biogeochemistry following the methods of Jay *et al.* (2023). We used the hillslope hydrology configuration to explicitly represent the lateral redistribution of water due to topography at the scale of a 'representative' hillslope, with three hydrologically connected columns (two upslope columns for moist and dry meadows and one downslope 'lowland' column for wet meadow) that are interconnected by surface and subsurface lateral flow (see Supporting Information Fig. S1).

To better represent conditions at this high alpine site, including strong winds that redistribute snow (Winstral *et al.*, 2002; Erickson *et al.*, 2005), we made modifications to winter precipitation in CLM that result in maximum snow depths that align with periodic snow depth measurements collected across the Saddle grid (D. Walker *et al.*, 2022). Specifically, leeward (east-facing) slopes accumulate the deepest winter snowpack and support more productive moist meadow communities, compared with windward (west-facing) slopes that accumulate little snow and support less productive dry meadow communities. When air temperatures were below 0°C we modified precipitation as follows: moist meadow columns received 100% of observed Saddle precipitation, wet meadow columns received 75% of observed precipitation, and dry meadow columns received only 10% of observed precipitation in the winter (increasing to 25% in the spring), and when air temperatures were above freezing all columns received the same precipitation as rain.

We also made modifications to soil properties that reflect observations from Niwot Ridge. These soil property data came from the National Ecological Observatory Network soil Megapit measurements (NEON, 2022; as in Lombardozzi *et al.*, 2023), with additional modifications to reflect local heterogeneity, indicating that wetter areas have deeper, more developed soils (Burns, 1980; see Table 1 for details). Broadly, (1) wet meadow columns had higher organic matter and clay content; (2) dry meadow soils had a lower water holding capacity (reflecting their rocky characteristics); and (3) all columns had a reduced dry surface layer thickness, which provides a primary control on soil evaporation (Swenson & Lawrence, 2014).

To generate initial conditions, including vegetation and soil C and N pools, we spun up all simulations for 200 yr in 'accelerated decomposition' mode by cycling over forcing data from 2008 to 2011. Soil and vegetation C and N pools were then allowed to equilibrate for another 100 yr (Lawrence *et al.*, 2019). We used observations of atmospheric data over the experimental period from 2008 to 2021 to run historical simulations with fixed CO_2 concentrations (409 ppm CO_2).

Floristic diversity: functional traits and phenology Before modifying plant trait values using data collected at the site, we ran a 'default' simulation that used the default CLM5 Arctic C_3 grass plant functional type (PFT) with no parameter modifications. We did not expect this default simulation with an 'out of the box' definition of a single PFT to capture the diversity of plant growth strategies that is common in tundra ecosystems. To better characterize tundra vegetation at Niwot Ridge, we subsequently modified PFT parameterizations to represent distinct tundra vegetation communities (as described in Jay *et al.*, 2023). Specifically, we created three distinct PFTs (using the Arctic C_3 grass PFT as the starting point) representing dry, moist, and wet meadow vegetation by modifying parameters related to foliar traits, plant hydraulics, and photosynthetic capacity to match vegetation growth strategies at our site (see Table 1 for default and modified parameter values). We modified specific leaf area (SLA) and foliar C : N ratios based on a synthesis of local site observations for moist, wet, and dry meadow (described in 'Foliar traits and phenology' in the Materials and Methods section). We then used observations from the site and values from CLM Arctic–boreal model development work (Fisk *et al.*, 1998; Birch *et al.*, 2021) to modify fine root to leaf allocation for each community (Table 1). We decreased two plant hydraulic stress parameters that represent maximum stem and root conductivity (Kennedy *et al.*, 2019) in the dry meadow in order to represent more conservative growth strategies. Finally, to better represent the relatively conservative growth strategies of alpine vegetation, we decreased two photosynthetic parameters, $jmaxb_0$ and $jmaxb_1$. These parameters specify the baseline proportion of N allocated for electron transport and the response of electron transport rate to light availability, respectively, in the mechanistic model of photosynthesis (leaf utilization of N for assimilation or LUNA; Ali *et al.*, 2016) used in CLM5.

In addition to functional traits, we modified several phenology parameters in our simulations using the phenometrics calculated

Table 1 Modifications to foliar, hydraulic, and photosynthetic parameters and soil properties in the Community Land Model (CLM) to better represent moist, wet, and dry alpine meadow environments.

Parameter	Description	Units	Moist meadow	Wet meadow	Dry meadow	Default
slatop[1,2]	Specific leaf area	$m^2\ g^{-1}$ C	0.0215	0.029	0.015	0.0402
leafcn[1,2]	Leaf C : N	g C g^{-1} N	19.6	17.7	18.5	28.03
ndays_on[3]	No. of days to complete leaf onset	d	21	28	25	10
crit_onset_gdd_sf[3]	Scale factor modifying GDD	Unitless	1	1	1.7	1
kmax[2]	Plant maximum conductance	mm H_2O mm^{-1} H_2O s^{-1}	2.42E-09	2.42E-09	2.30E-10	2.42E-09
krmax	Root maximum conductance	mm H_2O mm^{-1} H_2O s^{-1}	8.05E-11	8.05E-11	2.05E-11	8.05E-11
$jmaxb_0$	Baseline proportion of N for electron transport	Unitless	0.0225	0.0225	0.0225	0.0331
$jmaxb_1$	Response of electron transport rate to light availability	Unitless	0.1	0.1	0.1	0.1745
froot_leaf	New fine root C per new leaf C allocation	g C g^{-1} C	1.5	1.5	2	2
d_max	Dry surface layer thickness	mm	10	10	10	15
h_bedrock	Depth to bedrock	m	1.3	1	1	
wat_sat	Water saturation (porosity)	$m^3\ m^{-3}$			wat_sat/2	
organic[4]	Organic matter density	kg m^{-3}	80.7	107.6	80.7	
sand[4]	Percent sand	%	49.3	44.4	49.3	
clay[4]	Percent clay	%	12.7	14	12.7	

Default values specified in the parameter file are listed for comparison where available. C, carbon; GDD, growing degree days; N, nitrogen. Adapted from Jay *et al*. (2023).

[1]Values for each vegetation community from Spasojevic *et al*. (2013).

[2]Parameters that were modified in functional trait experiments to represent more resource-use conservative or acquisitive communities. See Supporting Information Table S1 for exact values used in experiments.

[3]Values for each vegetation community derived from Niwot Ridge phenocam green chromatic coordinate (GCC) data set (Elwood *et al*., 2022) and resulting phenometric calculations.

[4]Values based on National Ecological Observatory Network (NEON) Megapit (NEON, 2022).

from phenocam imagery for each community (described in 'Foliar traits and phenology' in the Materials and Methods section). As described in Jay *et al*. (2023), we calculated accumulated growing degree days (GDD; when surface soil temperatures > 0°C) before the start of leaf onset using 5 cm soil temperature observations from each plot and start of growing season dates from each community. We used these community-specific GDD values to modify a GDD scale factor in the CLM to incorporate the higher GDD accumulation required to trigger leaf out in the dry meadow (a 70% increase compared with moist and wet meadows). We also modified the length of the greenup period in our simulations (*ndays_on* parameter in the model; see Table S1) to reflect the observed number of days between leaf onset and peak greenness calculated for each vegetation community.

Model projections and uncertainty partitioning

Climate models typically consider uncertainty in the forced response of climate change that is generated from alternative scenarios of future greenhouse gas emissions (Hawkins & Sutton, 2009). To simulate uncertainty among two potential climate change scenarios and their effects on abiotic conditions, we extended our simulations to 2100 under the SSP2-4.5 and SSP3-7.0 scenarios (O'Neill *et al*., 2016). These represent medium and high emissions scenarios, respectively, with atmospheric CO_2 concentrations reaching 603 and 867 ppm by 2100. In CESM2, this scenario uncertainty resulted in 2.1°C and 3.4°C degrees of warming, respectively, in the gridcell that includes Niwot Ridge. To allow for a smooth transition between the observed meteorological record (2008–2021) and projected climate change scenarios simulated by CESM2, we used an anomaly forcing protocol (Wieder *et al*., 2015) following the methods of Jay *et al*. (2023). Briefly, the anomaly forcing protocol involves calculating mean monthly anomalies of the atmospheric state by subtracting CESM2 projections under SSP2-4.5 and SSP3-7.0 scenarios through the year 2100 from the climatological mean of the 'historic' baseline (2005–2014). These monthly anomalies were then added to observed meteorology (recycled over the observed record from 2008 to 2021) as a way to extend our simulations through 2100 under these two climate change scenarios. We note that this anomaly forcing protocol only represents a single model's representation of potential climate change trajectories in each of the SSP scenarios. Moreover, the coarse scale of a CESM gridcell (nominal one-degree resolution), relative to the scale of site observations, may underestimate rates of change in high elevation ecosystems. Despite these limitations, this approach provides opportunities to project a range of potential abiotic changes that tundra ecosystems at Niwot Ridge may experience through the end of this century.

To quantify uncertainty in potential biotic responses to climate change, we considered how shifts in the expression of plant functional traits may mediate ecological responses to these two climate change scenarios. To do this, we conducted plant trait experiments that included the control case (parameterized for each tundra vegetation community, as described above) as well as two additional cases where all three communities were shifted to have more resource-use conservative or acquisitive traits. To represent these shifts in resource acquisition strategies, we focused

on functional traits, modifying SLA, leaf C : N, and *kmax*, or plant maximum conductance, used here as a proxy for water use efficiency (see Table S1 for modified trait values used in these experiments), three traits that are important in shaping plant resource use strategies (Díaz *et al.*, 2016). Specifically, we increased SLA and *kmax* and decreased leaf C : N to represent more resource-acquisitive communities (and vice versa for more resource-use conservative communities; Table S1) based on their well-established relationships with the leaf economics spectrum, which extends to tundra ecosystems (Thomas *et al.*, 2020). We increased/decreased SLA and leaf C : N by 20% based on the variability in these traits observed at our site (Fig. 2) and increased/decreased *kmax* by 10% due to the high sensitivity of the model to this parameter.

We chose to vary plant functional trait responses toward more resource-conservative and acquisitive growth strategies this way because it reflects real uncertainty in the potential direction of alpine communities to environmental change. On one hand, more resource-conservative traits may be favored in tundra patches experiencing longer growing seasons but increasing soil moisture or thermal stress. By contrast, more resource-acquisitive traits may be beneficial in patches with higher resource availability throughout the growing season. Our simulated magnitude of trait change is also supported by previous work: Bjorkman *et al.* (2018) quantified biome-wide shifts in tundra functional traits based on measurements across 117 tundra sites over three decades and found that SLA increased by *c.* 5% per °C of warming. By modifying these parameters together, we aim to capture the range in biotic responses that could occur with climate change in each vegetation community. We also note that our experimental design represents an instantaneous shift in plant resource acquisition strategies. This simplification belies ecological uncertainties in the direction and rate of change that a particular tundra vegetation community may actually express. Our intent, therefore, is to broadly quantify uncertainties in climate change scenarios vs shifts in plant functional traits that may be experienced in tundra ecosystems. In CLM, leaf onset for the Arctic C_3 grass PFT is controlled by soil temperature (via growing degree days). Thus, phenological shifts are implicitly tied to the climate scenarios because warmer soils and earlier snowmelt advance greenup. Our experiments included shifts in functional trait parameters but not phenology parameters for this reason.

Using the two climate change scenarios and the three plant trait experiments described above, we ran six different CLM simulations from 2022 to 2100. We analyzed the outputs from these six simulations to partition the total uncertainty into plant trait and scenario contributions using a fixed effects analysis of variance for two groups following Bonan *et al.* (2019). We first calculated ensemble means for each model experiment and then calculated total uncertainty as the variance across the six-member ensemble. Scenario uncertainty was calculated as the variance of the multi-model means, and plant trait uncertainty was calculated as the mean of the multi-model variances for the SSP2-4.5 and SSP3-7.0 scenarios. We then determined the proportion of the total variance contributed by plant traits and climate scenarios for each year in our time series (2022–2100).

Results

Observed foliar traits and phenology

We found that community weighted mean functional traits and phenology differed significantly among moist, wet, and dry meadow alpine tundra vegetation. As expected, functional traits of dry meadow vegetation were more resource-use conservative, whereas moist and wet meadow vegetation tended to show more resource-acquisitive traits (Fig. 2). Specifically, dry meadow vegetation had lower SLA, higher leaf C : N, and higher $\delta^{13}C$ (a proxy for water use efficiency) compared with wet meadow vegetation. Counter to expectations, leaf C : N in the dry meadow was slightly lower than that of moist meadow, but SLA and $\delta^{13}C$ followed expected patterns (Fig. 2b). All pairwise comparisons between vegetation communities for each trait were statistically significant ($P < 0.001$).

Phenology, derived from GCC curves, also differed among vegetation communities (Fig. 3). Dry meadow vegetation greened up (Fig. 3b) and reached peak greenness (Fig. 3c) earlier compared with moist and wet meadow vegetation, though these differences were not statistically significant. Dry meadow also senesced later (Fig. 3d; $P < 0.05$) compared with moist meadow, resulting in a longer growing season than moist and wet meadow vegetation. Dry meadow also experienced a faster rate of spring greenup than moist and wet meadows (Fig. 3d; $P < 0.01$) and lower peak greenness (Fig. 3c; $P < 0.01$). By contrast, in the moist and wet meadows, where deeper snow delayed the onset and length of the growing season, median greenup day of year and rate of spring greenup values were very similar (Fig. 3b,d).

Model evaluation: comparing default and parameterized plant functional types

Using community-specific plant functional traits and phenology parameterizations (Figs 2, 3; Table 1) reduced biases in simulated plant productivity across all vegetation communities relative to the model default parameterization (Fig. 4). Flux tower measurements from Niwot Ridge suggest that annual GPP in the dry meadow/fellfield totals 114 ± 75 g C m^{-2} yr^{-1}. The default parameterization for Arctic C_3 grasses produced notably high annual GPP compared with historic simulations using observationally based parameterizations for dry meadow vegetation (1041 ± 188 g C m^{-2} yr^{-1} and 251 ± 39 g C m^{-2} yr^{-1} for default and calibrated model, respectively).

Additional lines of evidence suggest that vegetation-specific parameterizations improved simulated C-cycle dynamics across all vegetation communities. By modifying plant trait parameterizations to reflect resource acquisition strategies across tundra vegetation communities, parameterized model simulations captured the differences in ANPP. Specifically, productivity values increased with moisture and snow depth as in the observations (Fig. 4b). By contrast, in the default simulation, the dry meadow had the highest ANPP.

Incorporating community-specific phenology derived from phenocam imagery (GDD and number of days to complete leaf

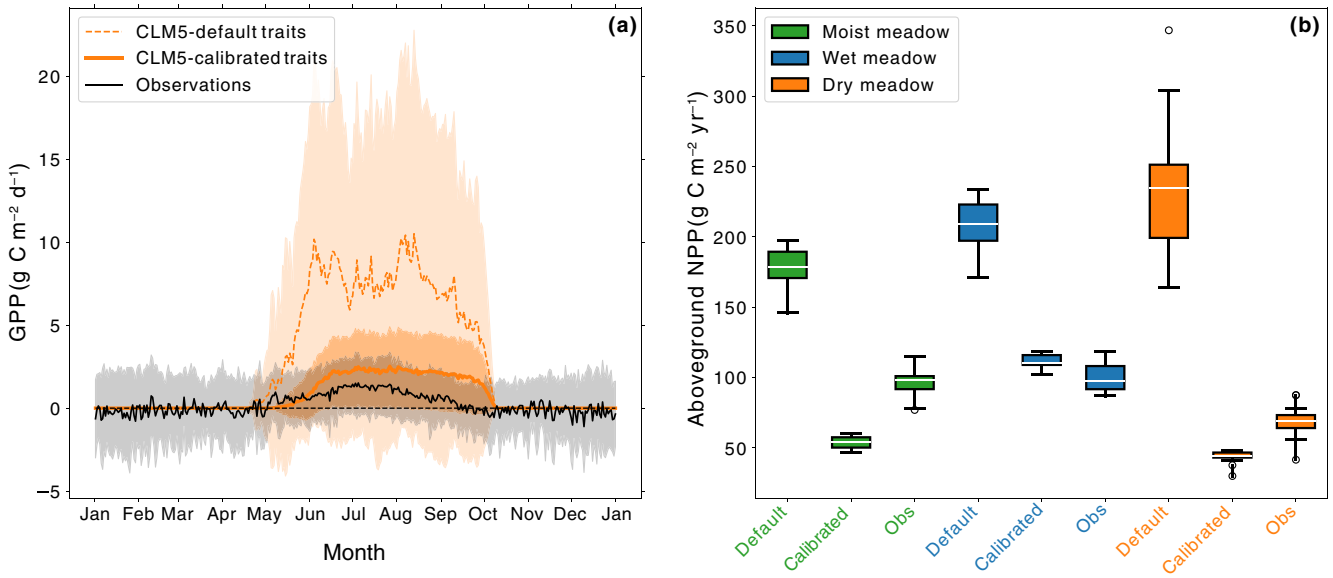

Fig. 4 Incorporating site-specific parameters for plant functional traits and phenology parameters greatly improves model estimates of productivity. (a) Mean annual climatology of gross primary productivity (GPP; averaged by day of year from 2008 to 2021) and (b) boxplots of mean annual aboveground net primary productivity (ANPP) in a 'default' CLM simulation with Arctic C_3 grasses compared with a simulation with calibrated, Niwot Ridge-specific parameterizations and Niwot Ridge observations (Obs) from: (a) eddy covariance measurements (black line) and (b) aboveground biomass clippings at the Saddle. Moist, wet, and dry meadows are shown in green, blue, and orange, respectively. Boxplot parameters are as follows: median (white lines), interquartile range (boxes), 1.5× interquartile range (whiskers), and outliers outside of this range (points).

onset) improved vegetation phenology in our simulations, but mismatches remain between modeled GPP and observed GCC curves (Fig. 5). Phenology observations from the site suggest that snowmelt controls the timing of greenup in the moist and wet meadows; the median start of season (sos) day of year was *c.* 175 and 177 in moist and wet meadows, respectively (Fig. 3b). Simulated snowmelt did not occur until day 190 and 175 on moist and wet meadow columns, respectively. Thus, greenup was delayed in the model relative to phenocam observations (Fig. 5a, b). In the dry meadow, where snow cover is thin and variable, we increased the number of GDD relative to the default value in CLM (see Table 1). As a result, the timing of greenup and senescence in our simulations closely matched the timing of phenocam GCC observations (Fig. 5c). In all three communities, the timing of the peak of the growing season was similar between our simulations and *in situ* observations as a result of modifying the number of days required to complete leaf onset, but the shape of the curves differed (Fig. 5). Specifically, GCC declined gradually throughout the growing season in the observations, while GPP was consistently high throughout the growing season in the CLM simulations until the critical daylength value was reached to trigger senescence (Fig. 5).

Model projection: plant functional trait vs scenario uncertainty

Building on our finding that there is significant functional trait variation within communities at the site (Fig. 2), we made additional trait modifications under our climate change scenarios that explore the uncertainty associated with a concurrent shift in trait expression within communities (e.g. toward a more resource-acquisitive or resource-conservative suite of traits). To examine how plant traits and climate scenario uncertainty affect tundra productivity under climate change, we extended our simulations to the year 2100 for moist, wet, and dry meadow vegetation under two different climate change scenarios (SSP2-4.5 and SSP3-7.0). For each of the three communities, we modified three parameters (SLA, leaf C : N, and *kmax*) to represent potential shifts toward more resource-use conservative or acquisitive growth strategies that may occur as a result of climate warming, and included these in our climate change projections. The anomaly forcing from CESM2 included increases of 2.1°C and 3.4°C in air temperature and 11.2% and 12.7% in precipitation by 2100 for SSP2-4.5 and SSP3-7.0, respectively, relative to the historical baseline (Table S2). These projected climate changes drove shifts in snowmelt, soil moisture and temperature, leaf onset timing, productivity, and runoff that varied across the topographically heterogeneous terrain (see Jay *et al.*, 2023 for more details). Here, we partition the variance in productivity changes that are projected across tundra vegetation types resulting from abiotic drivers (from climate change scenarios) and potential biotic responses to climate change (from potential shifts to more resource-conservative vs acquisitive plant functional traits).

With projected warming, we found that GPP and ANPP increased in the moist and wet meadows under both climate change scenarios. Changes in the dry meadow were more variable, with smaller increases in GPP and little or no change in ANPP (Figs 6, S2). In all future scenarios, positive GPP values occurred earlier and peak growing season GPP was higher compared with the historical simulation, reflecting both a phase shift

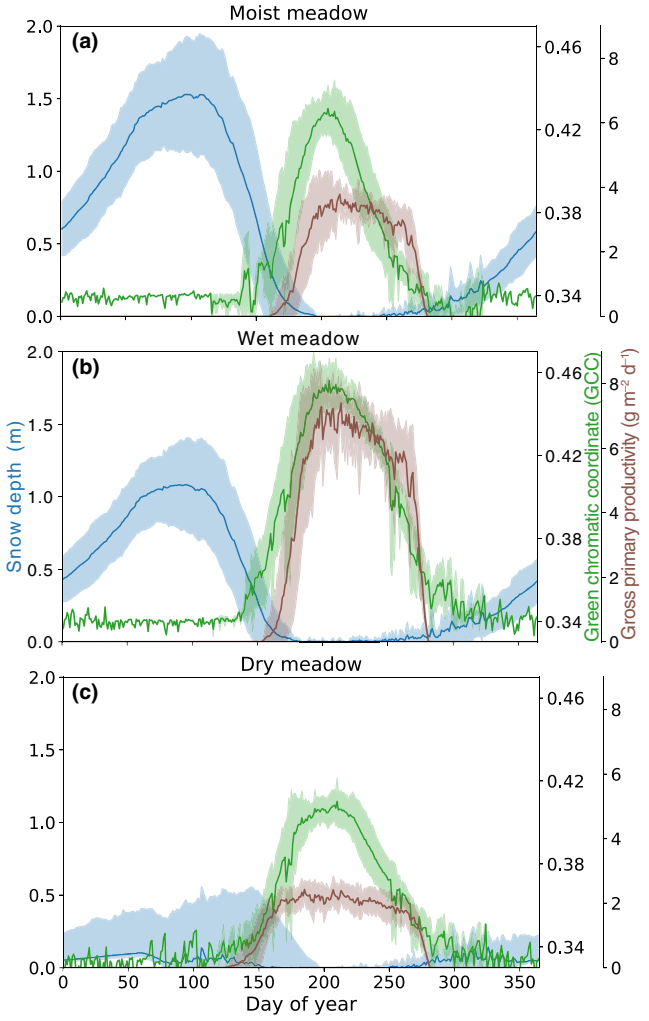

Fig. 5 Climatologies of simulated snow depth (m; blue lines) and gross primary productivity (GPP, g C m^{-2} d^{-1}; brown lines) from the Community Land Model (CLM) with Niwot Ridge-specific parameter values for vegetation functional traits and phenology, compared with phenocam-derived green chromatic coordinate (GCC, green lines) values. Panels include (a) moist meadow, (b) wet meadow, and (c) dry meadow. Climatological mean ± SD was calculated over the 13-yr data record for each vegetation community.

and amplification of productivity. This phenological shift resulted from earlier snowmelt (Fig. S3) and warmer soil temperatures that afforded longer growing seasons, especially under the SSP3-7.0 scenario.

The model also simulated amplification of daily GPP fluxes under the climate change scenarios from a combination of warmer temperatures and higher atmospheric CO_2 concentrations. These factors increase photosynthetic rates (Dong *et al.*, 2019) and water use efficiency (Keenan *et al.*, 2013), increasing leaf area index and daily GPP that is simulated by the model under the future scenarios. This amplification response was strongest in the moist and wet meadow, and under the SSP3.7-0 scenario compared with SSP2.4-5 (Figs 6a,b, S1a,b), but we found more muted C-cycle responses between the two scenarios in the dry meadow (Figs 6c, S1c). This response reflects the more favorable resource environments and resource-acquisitive traits found in the moist and wet meadow communities.

Besides these abiotically driven changes, we found a strong C-cycle response associated with potential shifts in functional traits of plant growth strategies. The shaded area for each climate scenario in Fig. 6 illustrates the magnitude of amplification uncertainty associated with shifts between resource-acquisitive vs conservative growth strategies. Specifically, shifts toward more resource-acquisitive traits (i.e. higher SLA, lower leaf C : N, and higher *kmax*) resulted in higher rates of GPP in all three community types and under both future climate scenarios. These changes were stronger for GPP than ANPP, particularly in simulations for dry meadow communities, and resource-acquisitive traits did not appear to increase ANPP (Fig. S2).

Variance partitioning analyses revealed that these shifts in plant functional traits represent a large source of uncertainty in future C-cycle responses, but the proportion of uncertainty attributed to traits varied among communities, over time, and by C-cycle metric (Fig. 7). Before 2060, trait uncertainty contributed a much greater proportion of variance in GPP than scenario uncertainty for all three vegetation communities (representing *c.* 70–100% of total uncertainty in the moist and wet meadows and *c.* 90–100% of total uncertainty in the dry meadow). After 2060, the contribution of functional trait uncertainty to total uncertainty decreased in the moist and wet meadows, ranging from 20% to 60% in most years, but remained relatively high and constant in the dry meadow through the end of this century (Fig. 7a–c).

There was much less variability in ANPP as a result of modifying plant resource acquisition strategies (Figs 6, S1). Accordingly, the proportion of variance in ANPP attributed to potential changes in plant traits was more variable than that of GPP, with trait uncertainty contributing anywhere from 10% to 100% of the variance depending on the year and community. Overall, climate scenario uncertainty contributed a larger proportion of total ANPP variance in the moist and wet meadows, particularly after 2060, when the trait uncertainty contributed < 20% (Fig. 7d–f). By contrast, ANPP variance in the dry meadow was still dominated by plant trait uncertainty until nearly the end of the century (*c.* 2080) when the contribution of scenario uncertainty increased, ranging from *c.* 40% to 65% (Fig. 7f).

Discussion

Our efforts to synthesize site-level observations into land model simulations with the CLM revealed significant community-level differences in functional traits and phenology among tundra vegetation. Incorporating this variability into ecosystem modeling efforts, where these communities would typically be represented by a single PFT, is critical to better understand how the ecosystem function of diverse tundra vegetation may shift under future climate conditions. Our findings reveal that potential plant functional trait shifts mediate ecosystem productivity responses to climate change. Specifically, we found that interacting shifts in the timing of leaf onset (driven by warming and earlier snowmelt

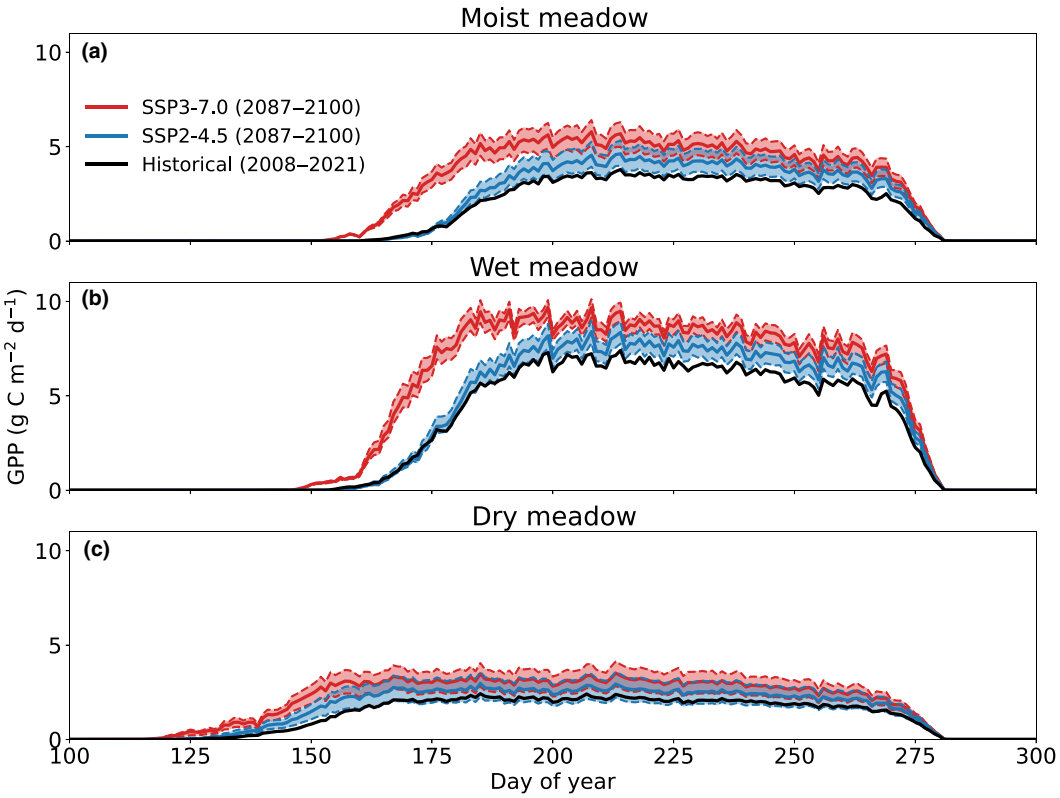

Fig. 6 Community Land Model (CLM) estimates of gross primary productivity (GPP) from historical (black) and Shared Socioeconomic Pathways (SSP) scenarios, including SSP2-4.5 (blue) and SSP3-7.0 (red). Panels show different vegetation communities, including (a) moist meadow, (b) wet meadow, and (c) dry meadow. Within each SSP scenario, the bold line represents the control simulation and the shading represents the variability due to trait experiments (from lower values with conservative traits to higher values with acquisitive traits, both represented by dashed lines). Values were averaged by day of year from 2008 to 2021 (historical) and 2087 to 2100 (SSP scenarios).

under climate scenarios) and functional traits led to both a phase shift and an amplification of ecosystem productivity (Figs 1, 6), suggesting that tundra ecosystems may be able to track future climate changes with shifts in functional traits. Notably, the effects of trait uncertainty on productivity were greater than those of uncertainty among climate scenarios until 2060 – and through the end of the century for dry meadow communities – indicating that this type of ecological uncertainty should be considered in climate change predictions. Our findings underscore the importance of understanding the direction and rate of biotic responses to this trait uncertainty in predicting ecosystem responses to future climate change.

Functional trait and phenological observations reduce model biases

We found that modifying key parameters corresponding to plant functional traits and phenology greatly improved the agreement of modeled C cycle metrics with observations in comparison to a default simulation. This was particularly evident in the dry meadow, which had the highest ANPP values in the default simulation, a pattern not supported by clip harvests from the site (Fig. 4b). This indicates that the default Arctic C_3 grass parameterization does not capture the more resource-conservative growth strategies that are characteristic of dry meadow vegetation. However, some biases remain in our calibrated results. Our simulations overestimated growing season GPP in the dry meadow (Fig. 4a), suggesting that simulated dry meadow vegetation does not experience adequate soil moisture stress, while underestimating ANPP by *c.* 30–40 g C m^{-2} yr^{-1} in dry and moist meadows, respectively (Fig. 4b). Because these observations are spatially distinct (with the clip harvests from the Saddle site and GPP from a drier south-facing site), they represent slightly different estimates of dry meadow communities; thus, our results suggest that our simulations are representing a reasonable middle ground of these different sites.

Our findings highlight the importance of incorporating field observations of plant traits to represent diverse vegetation growth strategies that are not captured by broad PFT groupings. Leveraging the hillslope hydrology configuration within CLM in combination with local plant functional trait and phenology observations allowed us to capture environmental gradients within tundra vegetation (see Jay *et al.*, 2023 for detailed model evaluation of snow, soil moisture and temperature, and productivity at this site). Our findings indicate that Arctic C_3 grass traits in CLM are not representative of tundra vegetation, which tends to be nutrient-use conservative (Reich, 2014) and adapted to extreme environmental conditions including short growing

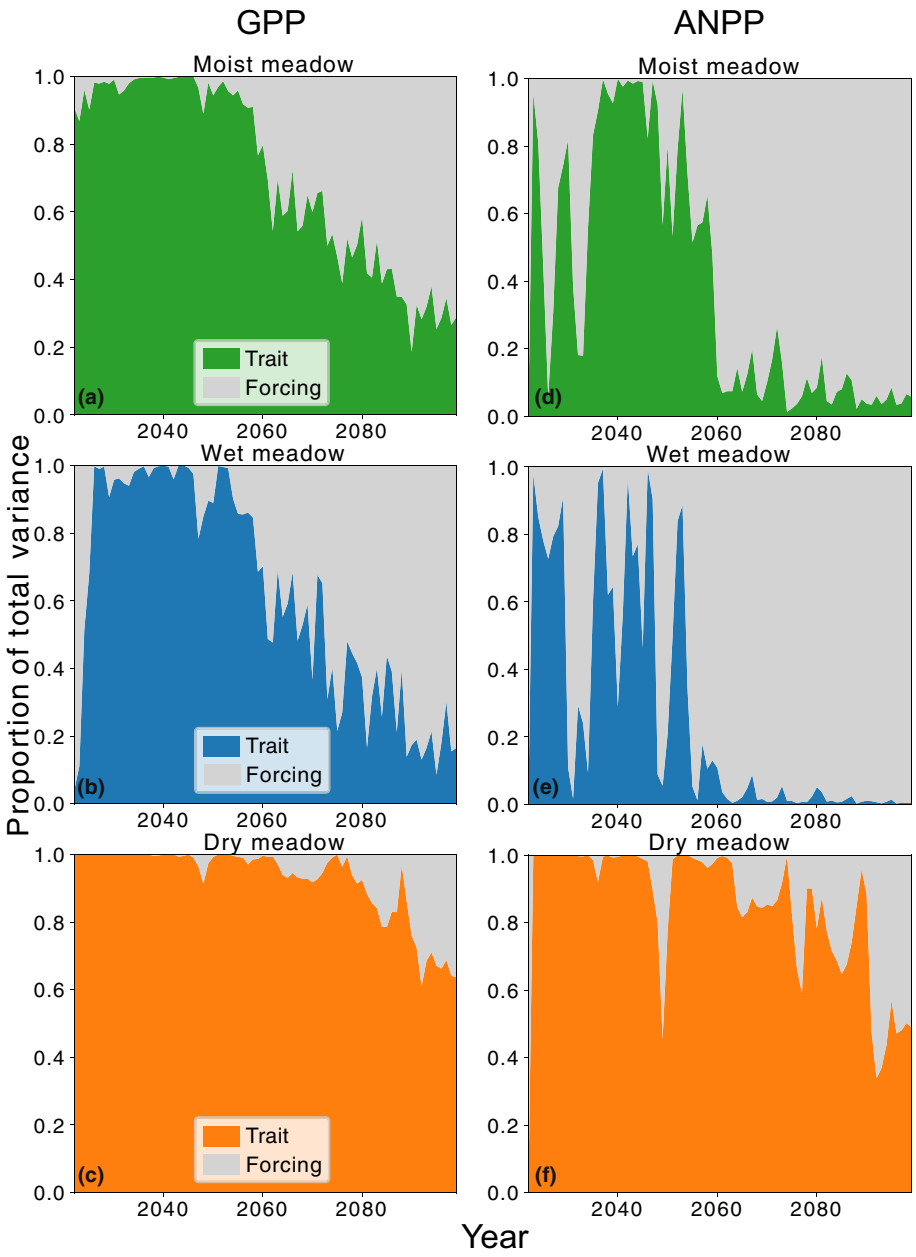

Fig. 7 Results of uncertainty partitioning analysis showing the proportion of total variance in productivity attributed to uncertainty in traits (green, blue, and orange for moist, wet, and dry meadows, respectively) and climate change scenario (gray) for each vegetation community. (a–c) Gross primary productivity (GPP), (d–f) aboveground net primary productivity (ANPP).

seasons, low temperatures, and nutrient limitation (Litaor *et al.*, 2008; Testolin *et al.*, 2021). While we modified our simulations based on field measurements available from our site, further modifications of PFTs, including less frequently measured parameters such as V_{cmax} and stomatal conductance (Bonan *et al.*, 2011; Hudiburg *et al.*, 2013), would further improve the representation of tundra ecosystems.

Incorporating community-specific leaf-out timing greatly improved modeled productivity estimates, and remaining biases in phenology varied among communities. The delay in greenup in simulated moist and wet meadows revealed limitations of our calibration of snow for different vegetation communities, where the spatially heterogeneous nature of available data sources at Niwot Ridge presents challenges for model calibration. However, colocated measurements of snow depth, vegetation phenology, plant traits, and ecosystem fluxes are rarely available at a single site, and we find that our simulations are broadly representative of the vegetation communities at this site despite the high spatial heterogeneity present in alpine terrain (Figs 4, 5; Opedal *et al.*, 2015). Phenology for seasonal-deciduous cold region PFTs in the CLM is driven primarily by temperature and daylength, where temperature triggers leaf onset when accumulated GDDs, soil temperature, and snow depth reach a critical value. Conversely, senescence and leaf litterfall occur when daylength is shorter than a critical value. This approach may be appropriate for energy-limited tundra vegetation, but it neglects the potential role of water stress that is characteristic of dry tundra communities. Moreover, the CLM phenology scheme was developed

from temperate deciduous forests (White *et al.*, 1997) and results in delayed predictions of leaf senescence as well as limited interannual variability in alpine vegetation (Figs 4a, 5; Jay *et al.*, 2023). Potential biases are exacerbated at high latitudes and elevations; in an evaluation of Arctic–boreal C-cycling in the CLM5, Birch *et al.* (2021) found that leaf onset and senescence were consistently late across PFTs. Analyses of phenocam images paired with microclimate measurements at Niwot Ridge suggest that greenup is strongly controlled by snowmelt and soil temperature, while senescence is controlled by both soil temperature and moisture (S. C. Elmendorf, unpublished). Taken together, our findings suggest that incorporating phenocam observations into modeling efforts and further refining phenology schemes to better represent variation among PFTs is critical for accurately predicting potential shifts in ecosystem productivity and C cycling.

Plant functional trait uncertainty outweighs scenario uncertainty

Overall, we found that differences among climate scenarios appear to control the onset of vegetation greenup and the timing of peak GPP in tundra ecosystems, leading to a phase shift in ecosystem productivity, while functional trait shifts primarily shaped GPP outcomes integrated over the entire growing season, leading to an amplification of productivity (Figs 1, 6). The magnitude of these phase shifts and amplifications, as well as the relative contributions of uncertainties to C-cycle metrics, however, varied among vegetation communities and over time. The contribution of plant trait uncertainty to total uncertainty decreased in the moist and wet meadows after the year 2060, but remained consistent in the dry meadow. This shift after 2060 suggests that the larger magnitude increases in temperature and atmospheric CO_2 concentrations occurring later in the century have a greater effect on productivity responses. Plant trait and climate scenario uncertainties also varied by C-cycle metric, where the contribution of trait uncertainty in ANPP was smaller and more variable compared with GPP. This difference between C-cycling metrics (GPP vs ANPP) is likely related to an increase in autotrophic respiration with warming (Drake *et al.*, 2016), which led to a higher contribution of scenario uncertainty to overall variance in ANPP.

In addition to the differences over time and by C-cycle metric, we observed variability in responses among vegetation communities across a snow accumulation gradient. This was unsurprising given the underlying abiotic heterogeneity that moderates exposure and rates of response to climate change at local scales in tundra ecosystems (e.g. Wieder *et al.*, 2017; Oldfather & Ackerly, 2019; Jay *et al.*, 2023). Growing season length and peak growing season GPP increased more between the medium and high emissions scenarios in the moist and wet meadows than in the dry meadow, where GPP did not increase substantially between the two scenarios (Fig. 6). This increase in growing season length reflects CLM assumptions that phenological shifts tightly track environmental change, as the environmental triggers that initiate leaf onset in the model are based on abiotic factors like snow depth and soil temperature. This earlier greenup under future climate scenarios is broadly consistent with experimental field manipulations that accelerated snowmelt at Niwot Ridge and generally found strong tracking of plant phenology to abiotic change (Rose-Person *et al.*, 2024). The differences among vegetation communities are likely due to differences in snow accumulation, where the timing of peak snow depth and snowmelt was much earlier in the moist and wet meadows under the higher emissions scenario (but with very little change in maximum snow depth; Fig. S3). This accelerated snowmelt increased soil temperatures, releasing moist and wet meadow vegetation from short growing season limitations and leading to a greater contribution of climate scenario uncertainty to total uncertainty in these communities compared with the dry meadow. By contrast, productivity of the dry meadow communities is more limited by soil moisture stress, rather than snow and soil temperature (Wieder *et al.*, 2017), and growth strategies are more resource-use conservative. Accordingly, productivity increased with shifts toward more resource-acquisitive traits, but the magnitude of this increase was likely limited by increased moisture stress under the higher emissions scenario.

Our model experiments applied an instantaneous shift in plant functional traits at the beginning of the climate change scenarios. This allowed us to examine the sensitivity of future productivity outcomes to climate change scenarios that may emerge from more resource-use acquisitive or conservative communities based on trait values that fall within the observed range of variability at our site (Fig. 2). However, our modeling experiments do not capture the direction or rate at which plant traits may shift with climate change, which is likely to vary across vegetation communities and environmental gradients (Oldfather *et al.*, 2024). For example, if abiotic change leads to increased resource availability, this should favor individuals with more resource-acquisitive traits, while abiotic changes that create more stressful conditions should favor those with more conservative growth strategies, but these patterns can be complicated by interacting global change factors and temporal variation in environmental drivers (Pacifici *et al.*, 2017; Huxley *et al.*, 2023; Henn *et al.*, 2024). These more nuanced vegetation responses are typically lacking in land modeling efforts that use static PFT parameterizations (Verheijen *et al.*, 2013). Similar limitations apply to phenological responses, which in CLM are tightly coupled to climate drivers; future work could explicitly assess phenological uncertainty, which has been shown to propagate into ecosystem carbon uptake (Migliavacca *et al.*, 2012). Advances in vegetation demographic models seek to provide computational tools to address these gaps through improved representation of ecologically relevant processes, for example by allowing disturbance and light competition to moderate interactions between plant functional traits and resource acquisition (Fisher *et al.*, 2015). Given the uncertainty in ecosystem responses to shifts in plant functional traits, explicit consideration of these mechanisms should be included in climate change predictions, particularly by incorporating vegetation demography and trait–environment relationships that can account for the functional responses of vegetation into land modeling efforts.

Conclusions

Taken together, our results suggest that uncertainties from potential changes in plant traits can exceed uncertainties from climate change scenarios in determining plant productivity responses to warming over the coming decades. The rate and direction of these trait responses will likely mediate the ability of vegetation to track (or lag) abiotic shifts driven by climate change (Fig. 1; Felton *et al.*, 2022). In our model experiments, the interacting effects of changes in plant traits and climate change scenarios led to both a phase and an amplification shift of future tundra productivity. However, the more stress-tolerant, dry meadow patches responded more slowly than the wetter, snowier moist and wet meadow patches, suggesting that spatial heterogeneity in snow accumulation will moderate whether communities may track, or lag, future climate changes. Accounting for this ecological uncertainty in future climate change projections is critical for better understanding terrestrial vegetation responses and their effects on ecosystem function.

Acknowledgements

This research was supported by National Science Foundation Grants DEB 1637686 and 2224439 to Niwot Ridge LTER. K. Jay was also supported in part by the Cooperative Institute for Research in Environmental Sciences (CIRES) at the University of Colorado Boulder and by the Environmental Data Science Innovation and Inclusion Lab (ESIIL) via the National Science Foundation award DBI 2153040. W. Wieder was also supported by NSF Grants 1926413 and 2120804. This material is based upon work supported by the NSF National Center for Atmospheric Research, which is a major facility sponsored by the U.S. National Science Foundation under Cooperative Agreement No. 1852977. We thank J. Morse, S. Aplet, and Niwot Ridge LTER staff for project support as well as members of the Suding Lab for helpful discussions and feedback on earlier versions of this manuscript. We also thank the anonymous reviewers for their feedback that improved the manuscript.

Competing interests

None declared.

Author contributions

KRJ, WRW and KNS conceived and designed the study. KRJ ran model experiments and conducted data analyses. SCE processed and analyzed phenocam data. MJS led the trait collection campaign. All authors contributed to data interpretation and writing.

ORCID

Sarah C. Elmendorf https://orcid.org/0000-0003-1085-8521
Katya R. Jay https://orcid.org/0000-0002-5098-3485
Marko J. Spasojevic https://orcid.org/0000-0003-1808-0048
Katharine N. Suding https://orcid.org/0000-0002-5357-0176
William R. Wieder https://orcid.org/0000-0001-7116-1985

Data availability

Computing and data storage resources, including the Derecho supercomputer, were provided by the Computational and Information Systems Laboratory (CISL) at NCAR. CLM code (CTSM Development Team, 2024) is available through the CTSM Github page and archived at: https://www.cesm.ucar.edu/models/clm. The CLM5 data analyzed in this manuscript (Jay & Wieder, 2025) are archived at NCAR's Geoscience Data Exchange (GDEX): doi: 10.5065/4gaq-xe30. Scripts for generating input data to drive our single-point simulations for Niwot Ridge as well as to run analyses and produce graphics are available on Zenodo at doi: 10.5281/zenodo.14680147.

References

Ali AA, Xu C, Rogers A, Fisher RA, Wullschleger SD, Massoud EC, Vrugt JA, Muss JD, McDowell NG, Fisher JB *et al.* 2016. A global scale mechanistic model of photosynthetic capacity (LUNA v.1.0). *Geoscientific Model Development* **9**: 587–606.

Beck PSA, Atzberger CG, Høgda KA, Johansen B, Skidmore AK. 2006. Improved monitoring of vegetation dynamics at very high latitudes: a new method using MODIS NDVI. *Remote Sensing of Environment* **100**: 321–334.

Billings WD, Mooney HA. 1968. The ecology of arctic and alpine plants. *Biological Reviews* **43**: 481–529.

Birch L, Schwalm CR, Natali S, Lombardozzi D, Keppel-Aleks G, Watts J, Lin X, Zona D, Oechel W, Sachs T *et al.* 2021. Addressing biases in Arctic–boreal carbon cycling in the Community Land Model v.5. *Geoscientific Model Development* **14**: 3361–3382.

Bjorkman AD, Myers-Smith IH, Elmendorf SC, Normand S, Rüger N, Beck PSA, Blach-Overgaard A, Blok D, Cornelissen JHC, Forbes BC *et al.* 2018. Plant functional trait change across a warming tundra biome. *Nature* **562**: 57–62.

Bonan GB. 2008. Forests and climate change: forcings, feedbacks, and the climate benefits of forests. *Science* **320**: 1444–1449.

Bonan GB, Lawrence PJ, Oleson KW, Levis S, Jung M, Reichstein M, Lawrence DM, Swenson SC. 2011. Improving canopy processes in the Community Land Model v.4 (CLM4) using global flux fields empirically inferred from FLUXNET data. *Journal of Geophysical Research* **116**: 1–22.

Bonan GB, Lombardozzi DL, Wieder WR, Oleson KW, Lawrence DM, Hoffman FM, Collier N. 2019. Model structure and climate data uncertainty in historical simulations of the terrestrial carbon cycle (1850–2014). *Global Biogeochemical Cycles* **33**: 1310–1326.

Burns SF. 1980. *Alpine soil distribution and development, Indian Peaks, Colorado Front Range.* Boulder, CO, USA: University of Colorado.

Burns SP, Maclean GD, Blanken PD, Oncley SP, Semmer SR, Monson RK. 2016. The Niwot Ridge Subalpine Forest US-NR1 AmeriFlux site – Part 1: Data acquisition and site record-keeping. *Geoscientific Instrumentation, Methods and Data Systems* **5**: 451–471.

Butler EE, Datta A, Flores-Moreno H, Chen M, Wythers KR, Fazayeli F, Banerjee A, Atkin OK, Kattge J, Amiaud B *et al.* 2017. Mapping local and global variability in plant trait distributions. *Proceedings of the National Academy of Sciences, USA* **114**: E10937–E10946.

Butterfield Z, Buermann W, Keppel-Aleks G. 2020. Satellite observations reveal seasonal redistribution of northern ecosystem productivity in response to interannual climate variability. *Remote Sensing of Environment* **242**: 111755.

Caine N. 1996. Streamflow patterns in the alpine environment of North Boulder Creek, Colorado Front Range. *Zeitschrift für Geomorphologie, Supplement* **104**: 27–42.

Cleland EE, Chuine I, Menzel A, Mooney HA, Schwartz MD. 2007. Shifting plant phenology in response to global change. *Trends in Ecology & Evolution* **22**: 357–365.

CTSM Development Team. 2024. ESCOMP/CTSM: ctsm5.2.005: Fix clm6_0 defaults and CESM testing issues, add tests to detect these problems (ctsm5.2.005). *Zenodo*. doi: 10.5281/zenodo.13324334.

Danabasoglu G, Lamarque J-F, Bacmeister J, Bailey DA, DuVivier AK, Edwards J, Emmons LK, Fasullo J, Garcia R, Gettelman A *et al.* 2020. The Community Earth System Model v.2 (CESM2). *Journal of Advances in Modeling Earth Systems* **12**: e2019MS001916.

Díaz S, Kattge J, Cornelissen JHC, Wright IJ, Lavorel S, Dray S, Reu B, Kleyer M, Wirth C, Colin Prentice I *et al.* 2016. The global spectrum of plant form and function. *Nature* **529**: 167–171.

Dong Z, Driscoll CT, Campbell JL, Pourmokhtarian A, Stoner AMK, Hayhoe K. 2019. Projections of water, carbon, and nitrogen dynamics under future climate change in an alpine tundra ecosystem in the southern Rocky Mountains using a biogeochemical model. *Science of the Total Environment* **650**: 1451–1464.

Drake JE, Tjoelker MG, Aspinwall MJ, Reich PB, Barton CVM, Medlyn BE, Duursma RA. 2016. Does physiological acclimation to climate warming stabilize the ratio of canopy respiration to photosynthesis? *New Phytologist* **211**: 850–863.

Elwood KK, Smith JG, Elmendorf SC, Niwot Ridge LTER. 2022. Time-lapse camera (phenocam) imagery of sensor network plots, 2017 – ongoing, v.3. *Environmental Data Initiative*. doi: 10.6073/pasta/285918fbf5cc4bd2ed2c1241db9a1b2d.

Erickson TA, Williams MW, Winstral A. 2005. Persistence of topographic controls on the spatial distribution of snow in rugged mountain terrain, Colorado, United States. *Water Resources Research* **41**: 41.

Felton AJ, Shriver RK, Stemkovski M, Bradford JB, Suding KN, Adler PB. 2022. Climate disequilibrium dominates uncertainty in long-term projections of primary productivity. *Ecology Letters* **25**: 2688–2698.

Filippa G, Cremonese E, Migliavacca M, Galvagno M, Forkel M, Wingate L, Tomelleri E, Morra di Cella U, Richardson AD. 2016. PHENOPIX: a R package for image-based vegetation phenology. *Agricultural and Forest Meteorology* **220**: 141–150.

Fisher RA, Muszala S, Verteinstein M, Lawrence P, Xu C, McDowell NG, Knox RG, Koven C, Holm J, Rogers BM *et al.* 2015. Taking off the training wheels: the properties of a dynamic vegetation model without climate envelopes, CLM4.5(ED). *Geoscientific Model Development* **8**: 3593–3619.

Fisk MC, Schmidt SK, Seastedt TR. 1998. Topographic patterns of above- and belowground production and nitrogen cycling in alpine tundra. *Ecology* **79**: 2253–2266.

Funk JL, Larson JE, Ames GM, Butterfield BJ, Cavender-Bares J, Firn J, Laughlin DC, Sutton-Grier AE, Williams L, Wright J. 2017. Revisiting the Holy Grail: using plant functional traits to understand ecological processes. *Biological Reviews* **92**: 1156–1173.

Hawkins E, Sutton R. 2009. The potential to narrow uncertainty in regional climate predictions. *Bulletin of the American Meteorological Society* **90**: 1095–1108.

He N, Yan P, Liu C, Xu L, Li M, Van Meerbeek K, Zhou G, Zhou G, Liu S, Zhou X *et al.* 2023. Predicting ecosystem productivity based on plant community traits. *Trends in Plant Science* **28**: 43–53.

Henn JJ, Anderson KE, Brigham LM, Bueno De Mesquita CP, Collins CG, Elmendorf SC, Green MD, Huxley JD, Rafferty NE, Rose-Person A *et al.* 2024. Long-term alpine plant responses to global change drivers depend on functional traits. *Ecology Letters* **27**: e14518.

Hooper DU, Chapin FS, Ewel JJ, Hector A, Ichausti P, Lavorel S, Lawton JH, Lodge DM, Loreau M, Naeem S. 2005. Effects of biodiversity on ecosystem functioning: a consensus of current knowledge. *Ecological Monographs* **75**: 3–35.

Hudiburg TW, Law BE, Thornton PE. 2013. Evaluation and improvement of the Community Land Model (CLM4) in Oregon forests. *Biogeosciences* **10**: 453–470.

Huxley JD, Spasojevic MJ. 2021. Area not geographic isolation mediates biodiversity responses of alpine refugia to climate change. *Frontiers in Ecology and Evolution* **9**: 633697.

Huxley JD, White CT, Humphries HC, Weber SE, Spasojevic MJ. 2023. Plant functional traits are dynamic predictors of ecosystem functioning in variable environments. *Journal of Ecology* **12**: 2597–2613.

Jay KR, Wieder WR. 2025. *Single-point CLM simulations at Niwot Ridge, CO with anomaly forcing (v.1.0)* [Dataset]. National Center for Atmospheric Research (NCAR) Geoscience Data Exchange. doi: 10.5065/4gaq-xe30.

Jay KR, Wieder WR, Swenson SC, Knowles JF, Elmendorf SC, Holland-Moritz H, Suding KN. 2023. Topographic heterogeneity and aspect moderate exposure to climate change across an alpine tundra hillslope. *Journal of Geophysical Research: Biogeosciences* **128**: e2023JG007664.

Keenan TF, Hollinger DY, Bohrer G, Dragoni D, Munger JW, Schmid HP, Richardson AD. 2013. Increase in forest water-use efficiency as atmospheric carbon dioxide concentrations rise. *Nature* **499**: 324–327.

Kennedy D, Swenson S, Oleson KW, Lawrence DM, Fisher R, Lola da Costa AC, Gentine P. 2019. Implementing plant hydraulics in the Community Land Model, v.5. *Journal of Advances in Modeling Earth Systems* **11**: 485–513.

Kittel TGF, Williams MW, Chowanski K, Hartman M, Ackerman T, Losleben M, Blanken PD. 2015. Contrasting long-term alpine and subalpine precipitation trends in a mid-latitude North American mountain system, Colorado Front Range, USA. *Plant Ecology and Diversity* **8**: 607–624.

Knowles JF. 2022a. *AmeriFlux BASE US-NR3 Niwot Ridge Alpine (T-Van West), v.3-5, AmeriFlux AMP* (Dataset). doi: 10.17190/AMF/1804491.

Knowles JF. 2022b. *AmeriFlux BASE US-NR4 Niwot Ridge Alpine (T-Van East), v.3-5, AmeriFlux AMP* (Dataset). doi: 10.17190/AMF/1804492.

Knowles JF, Blanken PD, Williams MW, Chowanski KM. 2012. Energy and surface moisture seasonally limit evaporation and sublimation from snow-free alpine tundra. *Agricultural and Forest Meteorology* **157**: 106–115.

Lawrence DM, Fisher RA, Koven CD, Oleson KW, Swenson SC, Bonan G, Collier N, Ghimire B, van Kampenhout L, Kennedy D *et al.* 2019. The Community Land Model v.5: description of new features, benchmarking, and impact of forcing uncertainty. *Journal of Advances in Modeling Earth Systems* **11**: 4245–4287.

Litaor MI, Williams M, Seastedt TR. 2008. Topographic controls on snow distribution, soil moisture, and species diversity of herbaceous alpine vegetation, Niwot Ridge, Colorado. *Journal of Geophysical Research: Biogeosciences* **113**: G02008.

Lombardozzi DL, Wieder WR, Sobhani N, Bonan GB, Durden D, Lenz D, SanClements M, Weintraub-Leff S, Ayres E, Florian CR *et al.* 2023. Overcoming barriers to enable convergence research by integrating ecological and climate sciences: the NCAR-NEON system v.1. *Geoscientific Model Development* **16**: 5979–6000.

Madani N, Kimball JS, Ballantyne AP, Affleck DLR, van Bodegom PM, Reich PB, Kattge J, Sala A, Nazeri M, Jones MO *et al.* 2018. Future global productivity will be affected by plant trait response to climate. *Scientific Reports* **8**: 2870.

Migliavacca M, Sonnentag O, Keenan TF, Cescatti A, O'Keefe J, Richardson AD. 2012. On the uncertainty of phenological responses to climate change, and implications for a terrestrial biosphere model. *Biogeosciences* **9**: 2063–2083.

Moritz C, Agudo R. 2013. The future of species under climate change: resilience or decline? *Science* **341**: 504–508.

Morse JF, Niwot Ridge LTER. 2022. Climate data for saddle catchment sensor network, 2017 – ongoing, v.4. *Environmental Data Initiative*. doi: 10.6073/pasta/598894834ae61d7550c30da06565.

Mott R, Vionnet V, Grünewald T. 2018. The seasonal snow cover dynamics: review on wind-driven coupling processes. *Frontiers in Earth Science* **6**: 197.

National Ecological Observatory Network (NEON). 2022. *Soil physical and chemical properties, Megapit*. NEON. doi: 10.48443/stbf-bh38.

National Oceanic and Atmospheric Administration (NOAA). 2021. *U.S. Climate Reference Network (USCRN) station 14W (40° 02′ N, 105° 32′ W) subhourly data*. National Centers for Environmental Information. [WWW document] URL https://www.ncei.noaa.gov/pub/data/uscrn/products/subhourly01/.

O'Neill BC, Tebaldi C, van Vuuren DP, Eyring V, Friedlingstein P, Hurtt G, Knutti R, Kriegler E, Lamarque J-F, Lowe J *et al.* 2016. The Scenario Model Intercomparison Project (ScenarioMIP) for CMIP6. *Geoscientific Model Development* **9**: 3461–3482.

Oldfather MF, Ackerly DD. 2019. Microclimate and demography interact to shape stable population dynamics across the range of an alpine plant. *New Phytologist* **222**: 193–205.

Oldfather MF, Elmendorf SC, Van Cleemput E, Henn JJ, Huxley JD, White CT, Humphries HC, Spasojevic MJ, Suding KN, Emery NC. 2024. Divergent community trajectories with climate change across a fine-scale gradient in snow depth. *Journal of Ecology* **112**: 126–137.

Opedal ØH, Armbruster WS, Graae BJ. 2015. Linking small-scale topography with microclimate, plant species diversity and intra-specific trait variation in an alpine landscape. *Plant Ecology and Diversity* **8**: 305–315.

Pacifici M, Visconti P, Butchart SHM, Watson JEM, Cassola FM, Rondinini C. 2017. Species' traits influenced their response to recent climate change. *Nature Climate Change* **7**: 205–208.

Rantanen M, Karpechko AY, Lipponen A, Nordling K, Hyvärinen O, Ruosteenoja K, Vihma T, Laaksonen A. 2022. The Arctic has warmed nearly four times faster than the globe since 1979. *Communications Earth & Environment* **3**: 1–10.

Reich PB. 2014. The world-wide 'fast–slow' plant economics spectrum: a traits manifesto. *Journal of Ecology* **102**: 275–301.

Rose-Person A, Spasojevic MJ, Forrester C, Bowman WD, Suding KN, Oldfather MF, Rafferty NE. 2024. Early snowmelt advances flowering phenology and disrupts the drivers of pollinator visitation in an alpine ecosystem. *Alpine Botany* **134**: 141–150.

Shipley B, Lechowicz MJ, Wright I, Reich PB. 2006. Fundamental trade-offs generating the worldwide leaf economics spectrum. *Ecology* **87**: 535–541.

Spasojevic MJ, Bowman WD, Humphries HC, Seastedt TR, Suding KN. 2013. Changes in alpine vegetation over 21 years: are patterns across a heterogeneous landscape consistent with predictions? *Ecosphere* **4**: art117.

Spasojevic MJ, Suding KN. 2012. Inferring community assembly mechanisms from functional diversity patterns: the importance of multiple assembly processes. *Journal of Ecology* **100**: 652–661.

Spasojevic MJ, Weber S, Niwot Ridge LTER. 2022. *Niwot plant functional traits, 2008–2018.* v.3. Environmental Data Initiative. doi: 10.6073/pasta/1a06bcffa07e7aa2a4b674af4c427860 [accessed 12 November 2025].

Suding KN, Lavorel S, Chapin Iii FS, Cornelissen JHC, Díaz S, Garnier E, Goldberg D, Hooper DU, Jackson ST, Navas M-L. 2008. Scaling environmental change through the community-level: a trait-based response-and-effect framework for plants. *Global Change Biology* **14**: 1125–1140.

Svenning J-C, Sandel B. 2013. Disequilibrium vegetation dynamics under future climate change. *American Journal of Botany* **100**: 1266–1286.

Swenson SC, Clark M, Fan Y, Lawrence DM, Perket J. 2019. Representing intrahillslope lateral subsurface flow in the Community Land Model. *Journal of Advances in Modeling Earth Systems* **11**: 4044–4065.

Swenson SC, Lawrence DM. 2014. Assessing a dry surface layer-based soil resistance parameterization for the Community Land Model using GRACE and FLUXNET-MTE data. *Journal of Geophysical Research: Atmospheres* **119**: 10299–10312.

Testolin R, Carmona CP, Attorre F, Borchardt P, Bruelheide H, Dolezal J, Finckh M, Haider S, Hemp A, Jandt U *et al.* 2021. Global functional variation in alpine vegetation. *Journal of Vegetation Science* **32**: e13000.

Thomas HJD, Bjorkman AD, Myers-Smith IH, Elmendorf SC, Kattge J, Diaz S, Vellend M, Blok D, Cornelissen JHC, Forbes BC *et al.* 2020. Global plant trait relationships extend to the climatic extremes of the tundra biome. *Nature Communications* **11**: 1351.

Tilman D, Reich PB, Knops J, Wedin D, Mielke T, Lehman C. 2001. Diversity and productivity in a long-term grassland experiment. *Science* **294**: 843–845.

Verheijen LM, Brovkin V, Aerts R, Bönisch G, Cornelissen JHC, Kattge J, Reich PB, Wright IJ, van Bodegom PM. 2013. Impacts of trait variation through observed trait–climate relationships on performance of an Earth system model: a conceptual analysis. *Biogeosciences* **10**: 5497–5515.

Walker D, Morse J, Niwot Ridge LTER. 2022. Snow depth data for saddle snowfence, 1992 – ongoing, v.13. *Environmental Data Initiative.* doi: 10.6073/pasta/e4e426e4646bf69bf2dfea8bd2784ee9.

Walker M, Smith J, Humphries H, Niwot Ridge LTER. 2022. Aboveground net primary productivity data for Saddle grid, 1992 – ongoing, v.6. *Environmental Data Initiative.* doi: 10.6073/pasta/b0cdc0cf7c4442f1b2ffc569e9890968.

Walker MD, Wahren CH, Hollister RD, Henry GHR, Ahlquist LE, Alatalo JM, Bret-Harte MS, Calef MP, Callaghan TV, Carroll AB *et al.* 2006. Plant community responses to experimental warming across the tundra biome. *Proceedings of the National Academy of Sciences, USA* **103**: 1342–1346.

Walker MD, Walker DA, Theodose TA, Webber PJ. 2001. The vegetation: hierarchical species-environment relationships. In: Bowman WD, Seastedt TR, eds. *Structure and function of an alpine ecosystem: Niwot Ridge, Colorado.* Oxford, UK: Oxford University Press, 99–127.

Wang Q, Fan X, Wang M. 2016. Evidence of high-elevation amplification versus Arctic amplification. *Scientific Reports* **6**: 19219.

White MA, Thornton PE, Running SW. 1997. A continental phenology model for monitoring vegetation responses to interannual climatic variability. *Global Biogeochemical Cycles* **11**: 217–234.

Wieder WR, Cleveland CC, Lawrence DM, Bonan GB. 2015. Effects of model structural uncertainty on carbon cycle projections: biological nitrogen fixation as a case study. *Environmental Research Letters* **10**: 044016.

Wieder WR, Kennedy D, Lehner F, Musselman KN, Rodgers KB, Rosenbloom N, Simpson IR, Yamaguchi R. 2022. Pervasive alterations to snow-dominated ecosystem functions under climate change. *Proceedings of the National Academy of Sciences, USA* **119**: e2202393119.

Wieder WR, Knowles JF, Blanken PD, Swenson SC, Suding KN. 2017. Ecosystem function in complex mountain terrain: combining models and long-term observations to advance process-based understanding. *Journal of Geophysical Research: Biogeosciences* **122**: 825–845.

Williams JW, Ordonez A, Svenning J-C. 2021. A unifying framework for studying and managing climate-driven rates of ecological change. *Nature Ecology & Evolution* **5**: 17–26.

Williams MW, Bardsley T, Rikkers M. 1998. Overestimation of snow depth and inorganic nitrogen wetfall using NADP data, Niwot Ridge, Colorado. *Atmospheric Environment* **32**: 3827–3833.

Winstral A, Elder K, Davis RE. 2002. Spatial snow modeling of wind-redistributed snow using terrain-based parameters. *Journal of Hydrometeorology* **3**: 524–538.

Wright IJ, Reich PB, Westoby M, Ackerly DD, Baruch Z, Bongers F, Cavender-Bares J, Chapin T, Cornelissen JHC, Diemer M *et al.* 2004. The worldwide leaf economics spectrum. *Nature* **428**: 821–827.

Supporting Information

Additional Supporting Information may be found online in the Supporting Information section at the end of the article.

Fig. S1 Overview photo and diagram of the Saddle site and associated vegetation communities at Niwot Ridge.

Fig. S2 Community Land Model (CLM) estimates of aboveground net primary productivity (ANPP) from historical (black) and Shared Socioeconomic Pathways (SSP) scenarios, including SSP2-4.5 (blue) and SSP3-7.0 (red).

Fig. S3 Community Land Model (CLM) estimates of snow depth (m) from historical (black) and Shared Socioeconomic Pathways (SSP) scenarios, including SSP2-4.5 (blue) and SSP3-7.0 (red).

Table S1 Plant functional trait values used to modify parameters for control, conservative, and acquisitive trait experiments for moist, wet, and dry meadows.

Table S2 Increase in mean annual temperature and mean annual precipitation between the historical simulation (averaged over 200–2021) and each of the two SSP–RCP scenarios (averaged over 2087–2100).

Please note: Wiley is not responsible for the content or functionality of any Supporting Information supplied by the authors. Any queries (other than missing material) should be directed to the *New Phytologist* Central Office.